A Lagrangian model for soil water dynamics during rainfall driven conditions

Erwin Zehe[1] and Conrad Jackisch[1]

1) Karlsruhe Institute of Technology (KIT)

Abstract:

Within this study we propose a stochastic approach to simulate soil water dynamics in the unsaturated zone by using a non-linear, space domain random walk of water particles. Soil water is represented by particles of constant mass, which travel according to the Itô form of the Fokker Planck equation. The model concept builds on established soil physics by estimating the drift velocity and the diffusion term based on the soil water characteristics. A naive random walk, which assumes all water particles to move at the same drift velocity and diffusivity, overestimated depletion of soil moisture gradients compared to a Richards' solver. This is because soil water and hence the corresponding water particles in smaller pore size fractions, are, due to the non-linear decrease of soil hydraulic conductivity with decreasing soil moisture, much less mobile. After accounting for this subscale variability of particle mobility, the particle model and a Richards' solver performed highly similar during simulated wetting and drying circles in three distinctly different soils. Both models were in very good accordance during rainfall driven conditions, regardless of the intensity and type of the rainfall forcing and the shape of the initial state. Within subsequent drying cycles the particle was typically slightly slower in depleting soil moisture gradients than the Richards' model.

Within a real world benchmark the particle model and the Richards' solver showed the same deficiencies in matching observed reactions of top soil moisture to a natural rainfall. The particle model performance, however, clearly improved after a straightforward implementation of rapid non equilibrium infiltration, which treats event water as different type of particle, which travel initially in the largest pore fraction at maximum velocity, and experience a slow diffusive mixing with the pre-event water particles within a characteristic mixing time. The proposed Lagrangian approach is hence a promising, easy to implement alternative to the Richards equation for simulating rainfall driven soil moisture dynamics, which offers straightforward opportunities to account for preferential, non-equilibrium flow.

Key words: soil water dynamics, random walk, Lagrange model, pre-event water, mobile and immobile water

1 INTRODUCTION

Only a tiny amount of water is stored in the unsaturated zone: with an estimated volume of about 16,500 km^3 (Dingman, 1994), soil moisture represents 0.05% of total fresh water. Nevertheless, this tiny storage amount exerts first order control on the partitioning of net radiation energy in latent and sensible heat flux (Kleidon and Renner, 2013a, b; Gayler et al., 2014; Turner et al., 2014) - maybe the key process in land surface atmosphere exchange. Crucially, soil moisture crucially controls CO_2 emissions of forest soils (Koehler et al., 2010), de-nitrification and related trace gas emissions into the atmosphere (Koehler et al., 2012) as well as metabolic transformations of pesticides (e.g. Holden and Fierer, 2005). Notwithstanding soil moisture controls splitting of rainfall into surface runoff and (preferential) infiltration (Zehe et al., 2007; Lee et al., 2007; Loos and Elsenbeer, 2011; Graeff et al., 2012; Bronstert et al., 2012; Zimmermann et al., 2013; Klaus et al., 2014). Soil water is furthermore a key factor limiting vegetation dynamics in savannah ecosystems (Saco et al., 2007; Tietjen et al., 2010).

Water storage in the unsaturated zone is controlled by capillary forces which increase nonlinearly with decreasing pore size, because water acts as a wetting fluid in soil (Horton and Jury, 2004). The standard approach to represent capillary and gravity controlled soil water dynamics is the Darcy-Richards equation in combination with suitable soil water characteristics. This continuum model essentially assumes that capillarity controlled diffusive fluxes dominate soil water dynamics under local equilibrium conditions even during rainfall driven conditions. Today we know that the assumptions of local equilibrium conditions (e.g. Hassanizadeh et al., 2002; Neuweiler et al., 2012) and a mainly diffusive flow are often not appropriate, particularly during rainfall events in structured soils. Rapid or preferential flow imply a strong local disequilibrium and imperfect mixing between a fast fraction of soil water, travelling in interconnected coarse pores or non-capillary macropores (Šimůnek et al., 2003; Wienhoefer et al. 2009; Klaus et al., 2013), and the slower diffusive flow in finer fractions of the pore space. As outlined in a couple of excellent review articles (e.g. Šimůnek et al., 2003; Beven and Germann, 2013), up to now many concepts have been proposed to overcome the inability of the Darcy – Richards concept to cope with not-well mixed or even non capillary, preferential flow. These concepts range from a) early stochastic convection (Jury, 1982), b) dual porosity and permeability approaches assuming overlapping and exchanging continua (Gerke and van Genuchten, 1993; van Schaik et al., 2014), to c) spatially explicit

representation of macropores as vertically and laterally connected flow paths (Vogel, 2006; Klaus and Zehe, 2010; Zehe et al., 2010a; Wienhoefer and Zehe, 2014) and d) non local formulations of the Richards equation (Neuweiler et al., 2012). Notwithstanding the listed short comings, the Darcy Richards concept works well when soil water dynamics are dominated by capillarity particularly during radiation driven conditions (Zehe et al., 2010b; Zehe et al., 2014). Furthermore, it would be foolish to mistake the limitations of the Richards equation with non-importance of capillary forces in soil. Without capillarity infiltrating rainfall would drain into groundwater bodies, leaving an empty soil as the local equilibrium state - there would be no soil water dynamics at all, probably even no terrestrial vegetation and the water cycle would operate in a complete different manner without capillary forces. Alternatives to the Darcy-Richards approach particularly for rainfall driven soil moisture dynamics are thus highly desirable, as long as they preserve the grain of "truth" about capillarity as underlying key control.

Here we propose such an alternative approach to simulate infiltration and soil moisture dynamics during and shortly after rainfall events in an effective, stochastic and yet physical way. Specifically, we hypothesise that infiltration and soil water flow during and shortly after rainfall events may be simulated by means of a non-linear random walk, representing soil water by a variable number of particles. To the best of our knowledge, similar Lagrangian approaches were proposed by Davies and Beven (2012) and taken much further by Ewen (1996b, a). In accordance with the latter approach our model concept is essentially built on capillarity by making use of soil physics and established soil water characteristics.

Particle tracking based on a random walk is usually employed for simulating advective-dispersive transport of solutes in the water phase, but not for the soil water phase itself (Delay and Bodin, 2001; Klaus and Zehe, 2011; Dentz et al., 2012). For linear problems, when neither the dispersion coefficient nor the drift term depend on solute concentration and thus particle density, a time domain representation of the random walk is favourable as it maximises computational efficiency (Dentz et al., 2012). Non-linear problems, such as transport of nonlinearly adsorbing solutes or the envisaged simulation of soil water dynamics, require a space domain, random walk, because the drift and diffusion term change non-linearly with changing particle density. Hence an integral treatment is in appropriate as the superposition principle is invalid for non-linear problems.

In the following we introduce the model concept and present different benchmarks to test its capability to simulate soil moisture dynamics during and shortly after rainfall events for equilibrium and non-equilibrium conditions. More specifically we a) detail the underlying theory and model implementation, b) reflect on obvious and non-obvious implications of treating water flow in a porous medium as a non-linear random walk and c) propose a straight forward way to treat non-equilibrium infiltration in section 2. Section 3 explains the model benchmarking a) against a model based on the Darcy-Richards concept for various soils, initial and boundary conditions as well as b) against soil moisture observations obtained in a rural loess catchment in Germany. After presenting the results in section 4, we close with discussion and conclusions in section 5.

2 THEORY AND MODEL IMPLEMENTATION

2.1 A random walk approach for diffusive water flow in the soil matrix

Our starting point is the Richards equation in the soil moisture based form.

$$\frac{\partial \theta}{\partial t} = \frac{\partial k(\theta)}{\partial z} + \frac{\partial}{\partial z}\left(D(\theta)\frac{\partial \theta}{\partial z}\right) \quad \text{(Eq.1)}$$
$$D(\theta) = k(\theta)\frac{\partial \psi}{\partial \theta}$$

θ [L^3/L^3] is the volumetric soil water content. Eq. (1) can be re-written in as,

$$\frac{\partial \theta}{\partial t} = \frac{\partial}{\partial z}\left[\frac{k(\theta)}{\theta}\theta \right] + \frac{\partial}{\partial z}\left(D(\theta)\frac{\partial \theta}{\partial z}\right) \text{ (Eq. 2.),}$$

and Eq. 2 can be further re-written into a divergence based form

$$\frac{\partial \theta}{\partial t} = \frac{\partial}{\partial z}\left[\frac{k(\theta)}{\theta}\theta - \frac{\partial D(\theta)}{\partial z}\theta \right] + \frac{\partial^2}{\partial z^2}\left(D(\theta)\theta\right) \text{ (Eq. 3).}$$

Equation 3 is formally equivalent to the Fokker-Planck equation. The volumetric soil water content θ [L^3/L^3] corresponds to the concentration C [M/L^3] in the advection diffusion equation; the first term corresponds to a drift/advection term $u(\theta) = k(\theta)/\theta - \partial D(\theta)/\partial z$ [L/T] characterizing downward advective water fluxes driven by gravity. The second term

corresponds to the dispersive/diffusive solute flux, by representing diffusive water movements driven by the soil moisture gradient and controlled by the diffusivity $D(\theta)$ [L^2/T] of soil water. D is the product of the hydraulic conductivity $k(\theta)$ [L/T] and the slope of the soil water retention curve $\frac{\partial\psi}{\partial\theta}$ [L]. This formal equivalence and the work of Ewen (1996 a, b) motivated the idea to simulate infiltration and soil water movement by a random walk of a large number of particles. The soil moisture profile at a given time and within a given spatial discretisation is represented by the spatial density of "water particles" at this time. Water particles are constant in mass and volume. The trajectory of a single particle within a time step Δt is described by the corresponding Langevin equation:

$$z(t+\Delta t) = -\left(\frac{k(\theta(t))}{\theta(t)} + \frac{\partial D(\theta(t))}{\partial z}\right)\cdot\Delta t + Z\sqrt{6\cdot D(\theta(t))\cdot\Delta t} \quad \text{(Eq. 4)}$$

With Z being a random number, uniformly distributed between [1,-1]. Or when using standard normally distributed random numbers, N, one obtains alternatively.

$$z(t+\Delta t) = -\left(\frac{k(\theta(t))}{\theta(t)} + \frac{\partial D(\theta(t))}{\partial z}\right)\cdot\Delta t + N\sqrt{2\cdot D(\theta(t))\cdot\Delta t} \quad \text{(Eq. 5)}$$

The term $\partial D(\theta)/\partial z$ corrects the drift term in the case of a spatial variable diffusion as recommended by (Kitanidis, 1994; Roth and Hammel, 1996; Michalak and Kitanidis, 2000; Elfeki et al., 2007; Uffink et al., 2012). The main difference to the usual linear random walk is that D and k depend on soil moisture and thus the water particle density. Here we parameterise this dependence by means of the van-Genuchten (1980) and Mualem (1976) model (Figure 1).

2.2 Challenges of the particle based approach

2.2.1 Non-linear dependence of D and k on particle density

The obvious implication of the non- linear dependence of the drift velocity and diffusion term on the soil water content is that a short time stepping in combination with at least a predictor corrector scheme is needed to account for the non-linear change of both parameters during an integration time step.

The non-obvious implication arises from the fact that the soil water retention curve reflects the cumulative pore size distribution of the soil (Jury and Horton, 2004) and the actual soil moisture reflects water that is stored among different size fractions of the wetted pore space. At first sight, one could expect an approach where all water particles in the pore space experience the same diffusion coefficient $D(\theta(t))$ and drift $k(\theta(t))/ \theta(t)$ to work well for high particle numbers. This straightforward approach is in analogy to the treatment of solutes in a random walk, where all solute particles in a flow field experience indeed the same dispersion, as they experience the same "average path length". Hence their diffusion step scales for all solute particles with the same coefficient. A closer look reveals, however, that it might be not that straightforward in the pore space, because water flow velocity decreases with decreasing pore size, which is reflected in the non-linear decrease in soil hydraulic conductivity with decreasing soil water content. This non-linear decrease implies that the water particles representing the actual soil water content $\theta(t)$ do not all travel at the same constant drift velocity $k(\theta(t))$ and diffusivity $D(\theta(t))$. In fact, only a small fraction of the particles, representing the water in the largest wetted pores, travels according to these values; the remaining water particles, representing water stored in smaller pores, are much less mobile. To account for this distribution of mobility the diffusive step in the water particle model cannot scale for all particles with same maximum $D(\theta(t))$, it needs to reflect the distribution of D within the different wetted pore sizes fraction (Figure 1). To achieve this, we subdivide the particles in a grid cell into N bins (for instance 800) and calculate k and D starting from the residual moisture content to the θ_r stepwise to $\theta(t)$ using a step with $\Delta\theta = (\theta(t) - \theta_r)/N$. The random walk step for particles within a given bin is hence as follows:

$$z_i(t+\Delta t) = -\left(\frac{k(\theta_r + i\cdot\Delta\theta)}{\theta(t)} + \frac{\partial D(\theta_r + i\cdot\Delta\theta)}{\partial z}\right)\cdot\Delta t + N\sqrt{2\cdot D(\theta_r + i\cdot\Delta\theta)\cdot\Delta t} \quad \text{(Eq. 6)}$$

$$i = 1,\ldots,N$$

Essentially, we propose that a correct random walk implementation needs to account for the different mobility of the water particles in different pore sizes in the outlined manner. Contrarily, we expect a "naive" execution of Eq. (5), assuming that all particles in a given grid element as equally mobile according to $k(\theta(t))$ and $D(\theta(t))$, to overestimate fluxes and depletion soil moisture gradients.

2.2.2 The necessity to operate at high particle numbers

Another challenge when treating water flow in a Lagrangian approach is that a much larger number of particles is necessary compared to random walk applications of solute transport. Why so? The latter treats cases when a solute invades a domain with a small or zero background concentration of this solute. The total solute mass in the system can thus be represented by the order of $10^4 – 10^5$ particles even in large, two-dimensional domains at a good signal-to-noise ratio (Roth and Hammel, 1996; Zehe et al,. 2001). In the case of soil water dynamics the "background concentration", i.e. the stored pre-event water mass in the soil profile, is much larger than the input signal of infiltrating event water. The particle number must thus be considerably increased to the order of 10^6 in a one dimensional domain, to ensure that the rainfall input is represented by a number of particles which is sufficiently high for a stochastic approach.

2.3 Equilibrium and non-equilibrium infiltration

Infiltration into the soil at a given $\theta(t)$ is represented as input of event water particles $N^{in}(t)$ into the upper model element, thereby changing the soil water content by $\Delta\theta$. Local equilibrium conditions, as assumed in the Darcy-Richards concept, imply that water infiltrates into the smallest non-wetted part of the pore space (as sketched in Figure 1). Consequently the random walk of the event and pre-event water particles in the largest wetted pores is determined by $D(\theta(t)+ \Delta\theta)$ and $k(\theta(t)+ \Delta\theta)$ (Figure 1).

A straightforward approach to account for non-equilibrium infiltration is to assume that event water enters into and travels in the coarsest pores of the soil, thereby wetting the path of minimum flow resistance. This implies that diffusive mixing from these coarse pores into the smallest non-wetted part of the pore space is much slower than the gravity driven downward flow. Non-equilibrium infiltration may hence be simulated, by assigning the saturated hydraulic conductivity k_s as drift term for "event water particles" and assuming small diffusive mixing, for instance the lower 5 or 10% quantile of $D(\theta)$. From the latter we specify the time scales for the event water to mix with the pre-event water as explained further in section 3.2.

2.4 Model implementation and execution

2.4.1 Model parameters, initial and boundary conditions

The proposed water particle model is coded in Matlab and requires in its simplest form the same parameters, initial and boundary conditions as a numerical solver of the Richards equation (soil hydraulic functions for the entire soil profile as well as a rainfall time series). Although the random walk itself does not require a spatial discretisation, we employ a grid to calculate particle densities and soil water contents during run time. The model is populated with the initial number of particles based on definitions of either soil moisture or matric potential of the profile and its selected spatial discretisation. The particle mass m [M] is equal to the integral water mass of the initial state divided by N. The spatial gradient of the diffusion coefficient in Eq. (6) can hence be estimated by means of a centered finite difference.

Initial positions of the pre-event water particles in a given grid cell are uniformly distributed. Infiltration or soil evaporation is represented as particle input $N^{in}(t)$ or loss $N^{out}(t)$ into/from the upper model element, by dividing the infiltrated/evaporated water mass in a time step by the particle mass. Infiltrating particles start at z=0. Depending on the selected lower boundary condition, particles may drain freely from the domain (free drainage boundary), a fixed number of particles is kept (constant head boundary), or particles are not allowed to leave the domain (zero flux boundary).

For the implementation of non-equilibrium infiltration we treat event water particles as separate type of particles (Figure 1), similar to a different kind of solute that is not influenced by the pre-event water particles unless both fractions are well mixed. Shortly after infiltration we assume event particles to be mainly controlled by gravity; they travel according to $k(\theta_s)$ and experience a small diffusive motion characterized by $D_{mix.}$ D_{mix} determines the time scale at which pre-event and event water particles get mixed (compare Eq. 3). Non-equilibrium implies that the time scale for diffusive mixing t_{mix} is much larger than the time scale of advective transport t_{ad}, through a grid element Δz which implies the grid Peclet number being much larger than 1:

$$\frac{\Delta z k_s}{D_{mix}} = \frac{t_{mix}}{t_{ad}} >> 1$$

$$t_{mix} = \frac{(\Delta z)^2}{D_{mix}}; t_{ad} = \frac{\Delta z}{k_s} \quad \text{(Eq. 3).}$$

Based on this time scale mixing can be characterised by, for instance, using an exponential distribution (as proposed by Davies and Beven, 2012). In our study we selected an even simpler approach, assuming uniformly distributed mixing between the time when particle enter the domain and the mixing time. This approach maximises the entropy of the mixing process (Klaus et al., 2015) thereby minimizing the number of a priory assumption; because mixing of each particle is equally likely.

2.4.2 Time stepping and subscale variability of particle mobility

For model execution we choose a predictor corrector scheme: We predict the particle displacement for 0.5*Δt, based on k(θ(t)), D(θ(t)), update θ(t+0.5*Δt) based on the new particle density distribution and compute the full time step using k(θ(t+0.5*Δt)), D(θ(t+0.5*Δt)). As k(θ(t)) and D(θ(t)) are only available at the discrete nodes of the simulation grid, these are interpolated to the particle locations using inverse distance weights.

We tested two different approaches to cope with the above explained non-linear dependence of D and k on θ(t) and thus on particle density. The first, referred to as "full mobility mode", distributes D among the particles to resemble the shape of D between $D(\theta_r)$ and D(θ(t)) and of k between $k(\theta_r)$ to k(θ(t)) according to Eq. (6). To this end we subdivided the particles in a grid cell representing the actual soil water content θ(t) and the D and k curves in different numbers of bins, as shown in Figure 1, to estimate the sensitivity of N. This full mobility approach does, however, imply the need to calculate a large chunk of rather marginal displacements as k and D decline rather fast. The computational less extensive alternative is to calculate the displacement according to Eq. 2 exclusively for the fastest 10 or 20 % of water particles and assuming the remaining ones to be immobile. Of key interest in this context is also the question whether the fast mobile and the slow immobile particles fractions mix across the pores size fractions or not (Brooks et al., 2010). Mixing can be implemented by assigning the particles randomly to the different bins of during each time step D(θ), while no mixing

can be realised by always assigning the same particle to same pore size fraction/ "mobility class". Within our simulations we tested both options. The second option turned out to be clearly superior with respect to matching simulations with a Richards' solver. Alternatively, we implemented also the straightforward/naïve approach, where all particles in a grid cell travel according to the same diffusion coefficient and drift velocity.

3 MODEL BENCHMARKING

3.1 Particle model versus Richards equation

In a set of benchmarks we compared the particle model (PM) to a numerical solver of the Richards equation, which was also implemented using Matlab using the same predictor corrector scheme. We simulated wetting and drying cycles for three soils with rather different soil water characteristics (Table 1). The first is a sandy soil developed on limestone located in the Attert experimental basin in Luxembourg (Martinez-Carreras et al., 2010; Wrede et al., 2015). The second is a young highly porous and highly permeable soil on schistose periglacial deposits in the Attert basin, which predominantly consists of fine silt aggregates with relative coarse inter-aggregate pores. The third is a Calcaric Regosol on loess with a large fraction of medium size pores, which is located in the Weiherbach catchment in south western Germany.

These soils were exposed to simulated wetting and drying cycles summarized in Table 2, by combining block rains of different intensity with periods of no flux at the upper boundary. Thereby we compared two different initial soil moisture profiles: a uniform soil water content of 0.269 m^3m^{-3} and an s-shaped profile. The intensities of block rain events were selected to be small enough to avoid infiltration excess. Both models were operated at a constant grid size of 0.025 m and a coarser grid size of 0.05 m, to explore their related sensitivity. The model domain had a vertical extent of 1.5 m. Additionally, we run the particle model at different time steps to work out the upper limit for a feasible model execution. The initial number of particles was $N^{ini} = 10^6$ in all cases.

Additionally, we tested the model during a 3 h long drainage scenario starting from a bell shaped initial soil moisture profile. In the latter case the model domain was extended to a depth of 2.5 m. Last not least, we compared both models in the sandy soil using a 2h long convective rainfall event of 16 mm observed at a 6 minutes resolution in summer 2014 in the Attert catchment (Figure 1 d).

3.2 Real world benchmarks: moderate rainfall event on a loess soil

Additionally, we evaluated the particle model against moisture dynamics observed at the central meteorological station in the Weiherbach catchment (Zehe et al., 2001; Plate and Zehe, 2008). At this site past rainfall records and soil moisture records in 0.025, 0.1, 0.2, 0.3 and 0.4m are available at a 6 min resolution. We carefully selected a moderate nocturnal rainfall event, to avoid the influence of macropore flow and evaporation on wetting and subsequent drying. The event had a total amount of 4 mm with maximum rainfall intensity of 2 mm/h, started at the 9th of May at 1:15 and lasted until 4:15 a.m. The changes in soil moisture in the upper layers revealed a recovery of 90% of the rainfall water, which implies that a small fraction of the water might have bypassed the sensors.

Both models were operated at the fine spatial discretisation of 0.025 m. We set the number of pre-event particles to 10^6. The simulation period ranged from 0:05 until 5:45 a.m. at this day, to allow for a drainage period but to stop simulation before evaporation in the natural system kicked in. Hydraulic properties of the top and subsoil of the Calcaric Regosol are given in Table 3. Both models were initialised by assigning the observed soil moisture values, which increased from 0.18 m^3m^{-3} in 0.025 m to 0.33 m^3m^{-3} in 0.4 m depths, using inverse distance interpolation between the grid nodes. As no surface runoff occurred during this event, rainfall was treated as a flux boundary condition.

4 RESULTS

In the following we present final soil moisture profiles simulated with the Darcy - Richards and the particle model for selected runs and compare the temporal evolution of soil moisture profiles in form of 2d colour plots. In terms of computing time we noted no remarkable difference between the particle model and the Richards solver. This is because the code is implemented by relying almost exclusively on array operations, thereby avoiding time-consuming loops over all particles.

4.1 Particle model versus Richards equation

4.1.1 Sandy soil on lime stone

Figure 2 presents the final soil moisture profiles for both models for selected simulation experiments. Panel a) reveals that a treatment of soil moisture dynamics as naive random walk

(solid green line), when all particles travel according to $D(\theta(t))$ and $k(\theta(t))$, implies clearly - as expected - too fast mixing of event water particles into larger depths compared to the Richards equation (solid blue line). However, when we accounted for the different mobility of water particles in different pore sizes, by resembling the distribution of D and k according to Eq. (6) with a suitable number of bins (N), simulations with the particle model converge quickly converge to the simulations with the Richards equation. While a simulation with N = 10 bins shows still considerably differences to the Richards equation, a simulation with N = 50 bins provides already a much better match. When operating the particle model according to Eq. 6 using N = 800 bins, the model performed highly similar to the Richards equation for all simulation experiments. This can be deduced from panels b) and c) in Figure 2, which show the simulated soil moisture profiles which evolved from a uniform and a s-shaped initial state after a block rain input of 20mm, respectively. Panel d) in Figure 2 additionally corroborates the similar performance of both models during a simulated 1h wetting and 2h drying cycle. The particle model slightly underestimates the depletion of the soil moisture gradient, which can be deduced from the small overshoot at the top of the profile and final profile and the slightly smaller values at a depth between 15 and 60 cm. For the sandy soil we also found in general a very good agreement between the "full mobility" particle model and a simulation assuming a mobile fraction of 20% (solid green line Figure 2 b).

Figure 3 (a1 and a2) presents a comparison of both models for two different grid sizes, during a simulation of a block rain of 40 mm in 1h. While the simulations with the different models at a grid size of 0.05 m were clearly different in the depth of 0.2 and 0.4 m, they performed nearly identical at the finer grid size. Stronger differences between the particle model and the Richards model occurred, however, at the end of a 3h long drainage experiment, which started from a bell shaped initial state (Figure 3 b1 and b2). Additional simulations without drift term in Eq. 6 and without gravity flux in the Richards equation performed in contrary nearly indistinguishable (not shown). This suggests that during drainage conditions gravity driven flow in the Richards model is slightly faster than in the particle model, which explains the slight upward shift of the corresponding soil moisture peak.

However, both model perform nearly identical during the simulation of the convective rainfall event, as corroborated by Figure 3 d and Figure 4 c and d. Maximum feasible time steps for the particle model in fast draining soils were 200 s, as corroborated by Figure 3 c. In this

context it is worth mentioning that the Richards solver already started oscillating at time steps larger than 40 s.

Figure 4 sheds light on differences in simulated soil moisture dynamics by providing the temporal evolution of simulated soil moisture profiles in the form of 2d colour plots. Figure 4 a and b corroborate that small differences between the particle model and the Richards solver arise mainly during the 2 h drainage period that follows on the 1h long wetting phase. However, these differences are small, as further corroborated by 2d colour plots of the simulated drainage experiment (Figure 4 e and f). Both models perform highly similar during wetting periods in form of block rains (Figure 4 a and b) or during simulation of natural rainfall events (Figure 4 c and d).

We may hence state that the particle model might be not suited for long term simulations in coarse grained, fast draining soils during non-driven conditions. It appears however as a feasible alternative to the Richards equation for simulation of rainfall driven soil moisture dynamics in these soils.

4.1.2 Young silty soil on schist

Simulations of soil water dynamics for the young silty soil on schist, revealed again a highly similar performance of the Richards equation and the full mobility particle model. This is corroborated by Figure 5 for a simulated block rain of 20 mm in 1h (Panel a) and subsequent drying of 2h duration (Panel b). Both models perform also highly similar when starting with an s-shape initial soil moisture profile (Panel c) and during a 40 mm block rain (Panel d). During the latter case small differences occurred mainly close to the soil surface as shown for the final state (Figure 5 d) and the course of the simulation (Figure 6 c and d).

Again the particle model was slightly less efficient in depleting soil moisture gradients during longer drainage periods. This is corroborated by the overestimation of topsoil moisture simulated with the particle model compared to the benchmark based on the Richards equation (Figure 5 c) and the corresponding colour plot in Figure 6 a and b). The differences between simulations of the particle model operated in the full mobility mode and at a mobile fraction of 0.1 (Figure 5 panel c) were as small as in the sandy soil.

We may hence also state that the particle model might be a feasible alternative to the Richards equation for simulation of for rainfall driven soil moisture dynamics in soils which consists of fine aggregated, silty material. Compared to the Richards equation the particle model shows the same type of deficiency as during simulations for the sandy soil, a slightly too slow depletion of gradients due to a slightly too slow gravity flux, but less pronounced.

4.1.3 Calcaric Regosol on loess

Simulations of soil water dynamics in the either finer grained Calcaric Regosol on loess revealed again that both models performed highly similar, particularly when operating the particle model at a mobile fraction of 0.1. This is corroborated for 3h long block rain with a total amount of 15 mm (Figure 7a). While the particle model in the full mobility mode deviates from the benchmark model by a small underestimation of top soil moisture and an overestimation of the wetting front propagation to a depth of 0.25 m, the model with a mobile fraction of 0.1 yields an almost perfect match, also within a subsequent drying phase of 3h (as shown in Figure 7 c). The accordance between both models during a combined wetting and drainage phase starting from the s-shaped initial state was of similar quality, as can be deduced from the corresponding soil moisture profiles in Figure 7 (b and d) and the corresponding 2d colour plot of the simulated space-time soil moisture patterns (Figure 8 a and b).

We may hence state that the achievement of a very good and numerically efficient match of the Richards model required an operation of the particle model at a mobile fraction of 0.1. This is likely explained by the even finer pore sizes in the Calcaric Regosol, which is reflected in the corresponding air entry values in Table 1. This finding suggest that 90% of the water stored in soil this fined grained soil does not contribute to rainfall driven soil moisture dynamics, but compiles a rather immobile soil moisture stock.

4.2 Real world benchmark

The real world benchmark in the Calcaric Regosol revealed that the particle model operated at a mobile fraction of 0.1 and the Richards solver performed again almost identical. This can be deduced from the comparison of corresponding 2d colour plots of the simulated space-time soil moisture patterns in Figure 8 c and d as well as from the soil moisture profiles at the end of precipitation event (after 15000 s, Figure 9 a) and the end of the simulation (after 21000 s,

Figure 9 b). Both models overestimate the observed soil moisture increase in 0.025 m at both time steps but clearly underestimate the observed soil moisture increase in 0.1 m depth at the end of the simulation. Hence, although both models perform nearly identical, none of them does perform acceptable with respect to the observations.

A possible explanation for the overestimation of the soil moisture change in 0.025 m by the models, which is consistent with a non-closed water balance, is that a part of the rainfall water bypassed the measurement device due fast non-equilibrium infiltration in connected coarse pores. To test this idea, we performed additional simulations by treating infiltrating event water particles as a second particle type infiltrating into the largest pores, which uniformly mixed with the pre-event water particles within the time t_{mix}. Figure 9 c) and d) compare the event water content and total content (as the sum of pre-event and mixed water) for two different mixing times t_{mix}= 4004 (D_{mix} =1.5 10^{-7} m^2s^{-1}) and 17144 (D_{mix} =3.3 10^{-8} m^2s^{-1}), which correspond the lower 50 or 30 % quantiles of D(θ),respectively. Particularly, the model with the longer mixing time performed distinctly differently to the particle model, assuming well mixed infiltration. Event water infiltrates and bypasses the pre-event water to a depth of between 0.1 and 0.3 m in a clearly advective fashion. Related volumetric pre-event water contents peak at 0.04 m^3m^{-3} (Figure 9 c and d). Consequently, the rainfall input leaves a much weaker signal in the well mixed water fraction (Figure 10 c), reflecting those event water particles which diffusively travelled from the coarse pore fraction into the smallest non-wetted fraction. In case of the faster mixing most of the event water is already mixed with the pre-event water at the end of the rainfall event (Figure 9 c) and water is completed mixed at the end of the simulation (Figure 9 d). Consequently, the differences with the simulation assuming equilibrium infiltration are much less pronounced.

None of the selected mixing time scales did however yield a systematic better performance of the particle model, in a sense that the mixed water fraction, which we assumed to be in good contact with the TDR, better matched the observation at 0.025 m depth. This is corroborated for the final states in Figure 10 c) and d). We thus performed an additional model run assuming a diffusive mixing according to the 40 % quantile of D(θ), which corresponds to t_{mix} = 7800s (D_{mix} = 8.8 10^{-8} m^2s^{-1}). In this case the simulated well mixed water content was at both times and in good accordance with the observations at 0.025 m and 0.1 m. We may,

hence, state that the proposed explanation is feasible and that the particle model allows treatment of non-equilibrium infiltration in a straightforward manner.

5 DISCUSSION AND CONCLUSIONS

5.1 Subscale variability of water particles – the key to a reasonable performance of non-linear random walk

This study provides evidence that a non-linear, random walk of water particles is a feasible alternative to the Richards equation for simulating rainfall driven soil moisture dynamics in the unsaturated zone in an effective and yet physical manner. The model preserves capillarity as first order control and estimates the drift velocity and the diffusivity term based on the unsaturated soil hydraulic conductivity and the slope of the soil water retention curve. As expected, a naive random walk, when all particles in a grid element travel according to $k(\theta(t))$, $D(\theta(t))$, overestimated depletion of soil moisture gradients compared to the Richards solver within three different soils for all tested initial and boundary conditions. The key for improving the particle model performance was to account for the fact that soil water in different pore size fractions is not equally mobile. When accounting for this subscale variability in particle mobility in different pore sizes by resampling the D and k curves from their minimum to the actual values with a suitable numbers of bins (Eq. 6), the particle model performed in good to very good accordance with the Richards solver in three distinctly different soils. Both models were in very good accordance during rainfall driven conditions, regardless of the intensity and type of the rainfall forcing and the shape of the initial state.

Within subsequent drying cycles the particle was typically slightly slower in depleting soil moisture gradients than the Richards model. Test simulations corroborated that the likely reason for this is the fact that gravity driven flow in the Richards model is slightly faster than in the particle model. This reason is consistent with our finding that these differences are larger in the fast draining sandy soil with low retention properties than in the more fine grained soils.

5.2 Learning about inherent assumption and stepping beyond limitations of the Richards approach

Alternatively, we tested a less computational demanding approach, assuming only the 10 or 20% of the fasted particles to be mobile, while treating the remaining particles located in

smaller pores sizes as immobile. In the cases of the sandy soil and the silty soil a mobile fraction of 0.1 or 0.2 revealed almost identical results as the full mobility model. In the fine porous Calcarig Regosol the differences between the full mobility model and the model operated at a mobile fraction of 0.1 were slightly stronger. The mobile fraction mode was generally less dispersive then the full mobility model and particularly in better accordance with the Richards solver for all simulation experiments. Our simulations hence provide clear evidence that 90% of the water stored in fine porous cohesive soils does not contribute to rainfall driven soil moisture dynamics, but compiles a rather immobile soil moisture stock.

In this context we compared also the cases of perfect mixing and no mixing between mobile and immobile water particles between different time steps (as explained in section 2.4.2). The second option was clearly superior with respect to matching simulations with a Richards' solver, while the other yielded strong differences. We may thus state that the particle model is a suitable tool to "unmask" a) inherent implications of the Darcy-Richards concept on the fraction of soil water that actually contributes to soil water dynamics and b) the inherent very limited degrees of freedom for mixing between mobile and immobile water fractions. Our findings suggest, furthermore, that the idea of two separate water worlds, one supplying runoff the other supplying transpiration, which is advocated in Brooks et al. (2010), is a somewhat naïve interpretation of soil physics and the inherently low degrees of freedom water to mix across pores size fractions, than a real mystery.

In a real world benchmark the particle model matched simulations with the Richards solver again very well. However, both models clearly overestimated top soil wetting compared to observations, and underestimated wetting in 10 cm at the end of the simulation. An asset of the particle based approach is that the assumption of local equilibrium equation during infiltration may be easily ignored. Specifically, we did this to test the idea whether bypassing of a fast water fraction might explain the model bias in the topsoil. To this end infiltrating event water particles were treated as second particle type, which travel initially mainly gravity driven in the largest pore fraction at maximum drift, and yet experience a slow diffusive mixing with the pre-event water particles within a characteristic mixing time. Simulations with the particle model in the non-equilibrium mode performed evidently distinctly different in the topsoil, and were rather sensitive to the diffusion coefficient D_{mix} describing mixing of event water particles. When assuming D_{mix} equal to the 40% quantile of the $D(\theta)$ curve, the

mixed water fraction of the particle model was in good accordance with observed soil moisture changes at0.025 and 0.1 m depths after the rainfall and at the end of the simulation period.

Our findings are in line with the early findings of Ewen (1996b). The diffusive mixing term parameter D_{mix} is perhaps easier to interpret as the λ parameter Ewen (1996b) introduced to account for displacement of old water by new water particles, notwithstanding that displacement of pre-event water seems to play a key role in feeding macropore flow (Klaus et al, 2013; Klaus et al., 2014). Contrary to the exponential mixing term Davis and Beven (2012) introduced to stop rapid flow in the MIPs model, we used a uniform distribution which maximizes entropy of the mixed particles (Klaus et al., 2015).

5.3 Conclusions and Outlook

We conclude overall that the proposed non-linear random walk of water particles is an interesting alternative for simulating rainfall driven soil moisture dynamics in the unsaturated zone in an effective manner, which nevertheless preserves the influence of capillarity and makes use of established soil physics. The approach is easy to implement, even in two or three dimensions and fully mass conservative. The drawback is the required high density of particles, arising from the small ratio of event water to pre-event water in soil, which might become a challenge when working in larger domains and several dimensions. However, due to its simplicity the model is straight forward to implement on a parallel computer.

The approach has, however, compared to the Richards solver slight deficiencies during long term drainage phases, particularly in coarse grained, fast draining soils. One might hence find an adaptive model structure as favourable. During radiation driven conditions when water flow is slow and in local equilibrium, it is favorable to use to a Richards solver, because it works well and it is much more computationally efficient and treatment of for instance root water uptake is much more straightforward. During rainfall driven conditions, when time stepping needs to be in the order of minutes, due to the characteristic time scale of changes in rainfall intensity, we recommend to switch to the particle approach. Particularly also because the implementation of fast non-equilibrium infiltration and the separation of event and pre-event water is straight forward, for instance compared to a non-local formulation of the Richards equation (Neuweiler et al., 2012). In line with Ewen (1996) we hence regard particle

based models as particularly promising to deal with preferential transport of solutes (optionally also heat), and to explore transit time distributions in a forward mode.

We are aware, that the evidence we provided here is a somewhat tentative first step corroborate the flexibility of the particle based approach to include non-equilibrium flow and matrix flow in the same stochastic, physical framework. A much more exhaustive treatment of this issue is provided in a forthcoming study which presents and extension of the concept to a 2 dimensional domain with topologically explicit macropores and the test of concurring hypothesis to represent infiltration into macropores as well as macropore matrix interactions.

ACKNOWLEDGMENTS

This study contributes to and greatly benefited from the "Catchments As Organized Systems" (CAOS) research unit. We sincerely thank the German Research Foundation (DFG) for funding (FOR 1598, ZE 533/9-1). The authors acknowledge support by Deutsche Forschungsgemeinschaft and the Open Access Publishing Fund of Karlsruhe Institute of Technology (KIT). The service charges for this open access publication have been covered by a Research Centre of the Helmholtz Association. The code and the simulation projects underlying this study are freely available on request. We gratefully thank the three anonymous reviewers for their thoughtful comments, which were very helpful for improving the proposed model approach.

6 REFERENCES

Beven, K., and Germann, P.: Macropores and water flow in soils revisited, Water Resources Research, 49, 3071-3092, 10.1002/wrcr.20156, 2013.

Brooks, J. R., Barnard, H. R., Coulombe, R., and McDonnell, J. J.: Ecohydrologic separation of water between trees and streams in a mediterranean climate, Nature Geoscience, 3, 100-104, 10.1038/ngeo722, 2010.

Bronstert, A., Creutzfeldt, B., Graeff, T., Hajnsek, I., Heistermann, M., Itzerott, S., Jagdhuber, T., Kneis, D., Lueck, E., Reusser, D., and Zehe, E.: Potentials and constraints of different types of soil moisture observations for flood simulations in headwater catchments, Natural Hazards, 60, 879-914, 10.1007/s11069-011-9874-9, 2012.

Davies, J., and Beven, K.: Comparison of a multiple interacting pathways model with a classical kinematic wave subsurface flow solution, Hydrological Sciences Journal-Journal Des Sciences Hydrologiques, 57, 203-216, 10.1080/02626667.2011.645476, 2012.

Delay, F., and Bodin, J.: Time domain random walk method to simulate transport by advection-dispersion and matrix diffusion in fracture networks, Geophysical Research Letters, 28, 4051-4054, 10.1029/2001gl013698, 2001.

Dentz, M., Gouze, P., Russian, A., Dweik, J., and Delay, F.: Diffusion and trapping in heterogeneous media: An inhomogeneous continuous time random walk approach, Advances In Water Resources, 49, 13-22, 10.1016/j.advwatres.2012.07.015, 2012.

Dingman, S. L.: Physical hydrology, McMillan, New York, 575 pp., 1994.

Elfeki, A. M. M., Uffink, G. J. M., and Lebreton, S.: Simulation of solute transport under oscillating groundwater flow in homogeneous aquifers, Journal of Hydraulic Research, 45, 254-260, 2007.

Ewen, J.: 'Samp' model for water and solute movement in unsaturated porous media involving thermodynamic subsystems and moving packets .2. Design and application, Journal Of Hydrology, 182, 195-207, 10.1016/0022-1694(95)02926-5, 1996a.

Ewen, J.: 'Samp' model for water and solute movement in unsaturated porous media involving thermodynamic subsystems and moving packets .1. Theory, Journal Of Hydrology, 182, 175-194, 10.1016/0022-1694(95)02925-7, 1996b.

Gayler, S., Woehling, T., Grzeschik, M., Ingwersen, J., Wizemann, H.-D., Warrach-Sagi, K., Hoegy, P., Attinger, S., Streck, T., and Wulfmeyer, V.: Incorporating dynamic root growth enhances the performance of noah-mp at two contrasting winter wheat field sites, Water Resources Research, 50, 1337-1356, 10.1002/2013wr014634, 2014.

Gerke, H. H., and Van Genuchten, M. T.: A dual-porosity model for simulating the preferential movement of water and solutes in structured porous-media, Water Resources Research, 29, 305-319, 1993.

Graeff, T., Zehe, E., Blume, T., Francke, T., and Schröder, B.: Predicting event response in a nested catchment with generalized linear models and a distributed watershed model, Hydrological Processes, n/a-n/a, 10.1002/hyp.8463, 2012.

Hassanizadeh, S. M., Celia, M. A., and Dahle, H. K.: Dynamic effect in the capillary pressure-saturation relationship and its impacts on unsaturated flow, Vadose Zone Journal, 1, 38-57, 2002.

Holden, P. A. & N. Fierer (2005), Microbial processes in the vadose zone, Vadose Zone J., 4(1), 1-21.

Jury, W., and Horton, R.: Soil physics, John Wiley, Cambridge, U.K., 2004.

Jury, W. A.: Simulation of solute transport using a transfer function model Water Resources Res., 18, 363 - 368, 1982

627 Kitanidis, P. K.: Particle-tracking equations for the solution of the advection-dispersion
628 equation with variable-coefficients, Water Resources Research, 30, 3225-3227,
629 10.1029/94wr01880, 1994.
630 Klaus, J., and Zehe, E.: Modelling rapid flow response of a tile drained field site using a 2d-
631 physically based model: Assessment of "equifinal" model setups, Hydrological Processes,
632 24, 1595 – 1609, DOI: 10.1002/hyp.7687., 2010.
633 Klaus, J., and Zehe, E.: A novel explicit approach to model bromide and pesticide transport in
634 connected soil structures, Hydrology And Earth System Sciences, 15, 2127-2144,
635 10.5194/hess-15-2127-2011, 2011.
636 Klaus, J., Zehe, E., Elsner, M., Kulls, C., and McDonnell, J. J.: Macropore flow of old water
637 revisited: Experimental insights from a tile-drained hillslope, Hydrology And Earth System
638 Sciences, 17, 103-118, 10.5194/hess-17-103-2013, 2013.
639 Klaus, J., Zehe, E., Elsner, M., Palm, J., Schneider, D., Schroeder, B., Steinbeiss, S., van
640 Schaik, L., and West, S.: Controls of event-based pesticide leaching in natural soils: A
641 systematic study based on replicated field scale irrigation experiments, Journal Of
642 Hydrology, 512, 528-539, 10.1016/j.jhydrol.2014.03.020, 2014.
643 Klaus, J., Chun, K. P., McGuire, K. J., and McDonnell, J. J.: Temporal dynamics of
644 catchment transit times from stable isotope data, Water Resources Research, 51, 4208-
645 4223, 10.1002/2014wr016247, 2015.
646 Kleidon, A., and Renner, M.: A simple explanation for the sensitivity of the hydrologic cycle
647 to surface temperature and solar radiation and its implications for global climate change,
648 Earth System Dynamics, 4, 455-465, 10.5194/esd-4-455-2013, 2013a.
649 Kleidon, A., and Renner, M.: Thermodynamic limits of hydrologic cycling within the earth
650 system: Concepts, estimates and implications, Hydrology And Earth System Sciences, 17,
651 2873-2892, 10.5194/hess-17-2873-2013, 2013b.
652 Koehler, B., Zehe, E., Corre, M. D., and Veldkamp, E.: An inverse analysis reveals
653 limitations of the soil-co2 profile method to calculate co2 production and efflux for well-
654 structured soils, Biogeosciences, 7, 2311-2325, 10.5194/bg-7-2311-2010, 2010.
655 Koehler, B., Corre, M. D., Steger, K., Well, R., Zehe, E., Sueta, J. P., and Veldkamp, E.: An
656 in-depth look into a tropical lowland forest soil: Nitrogen-addition effects on the contents
657 of n2o, co2 and ch4 and n2o isotopic signatures down to 2-m depth, Biogeochemistry, 111,
658 695-713, 10.1007/s10533-012-9711-6, 2012.
659 Lee, H., Zehe, E., and Sivapalan, M.: Predictions of rainfall-runoff response and soil moisture
660 dynamics in a microscale catchment using the CREW model, Hydrol. Earth Syst. Sci., 11,
661 819-849, doi:10.5194/hess-11-819-2007, 2007.
662 Loos, M., and Elsenbeer, H.: Topographic controls on overland flow generation in a forest -
663 an ensemble tree approach, Journal Of Hydrology, 409, 94-103,
664 10.1016/j.jhydrol.2011.08.002, 2011.
665 Martinez-Carreras, N., Udelhoven, T., Krein, A., Gallart, F., Iffly, J. F., Ziebel, J., Hoffmann,
666 L., Pfister, L., and Walling, D. E.: The use of sediment colour measured by diffuse
667 reflectance spectrometry to determine sediment sources: Application to the attert river
668 catchment (luxembourg), Journal Of Hydrology, 382, 49-63,
669 10.1016/j.jhydrol.2009.12.017, 2010.
670 Michalak, A. M., and Kitanidis, P. K.: Macroscopic behavior and random-walk particle
671 tracking of kinetically sorbing solutes, Water Resources Research, 36, 2133-2146,
672 10.1029/2000wr900109, 2000.
673 Mualem, Y.: A new model for predicting the hydraulic conductivity of unsaturated porous
674 media, Water Resources Research, 12, 513-522, 1976.

675 Neuweiler, I., Erdal, D., and Dentz, M.: A non-local richards equation to model unsaturated
676 flow in highly heterogeneous media under nonequilibrium pressure conditions, Vadose
677 Zone Journal, 11, 10.2136/vzj2011.0132, 2012.
678 Plate, E., and Zehe, E.: Hydrologie und stoffdynamik kleiner einzugsgebiete: Prozesse und
679 modelle, in, Schweizerbart'sche Verlagsbuchhandlung (Nägele u. Obermiller), 366, 2008.
680 Roth, K., and Hammel, K.: Transport of conservative chemical through an unsaturated two-
681 dimensional miller-similar medium with steady state flow, Water Resources Research, 32,
682 1653-1663, 1996.
683 Saco, P. M., Willgoose, G. R., and Hancock, G. R.: Eco-geomorphology of banded vegetation
684 patterns in arid and semi-arid regions, Hydrology And Earth System Sciences, 11, 1717-
685 1730, 2007.
686 Šimůnek, J., Jarvis, N. J., van Genuchten, M. T., and Gärdenäs, A.: Review and comparison
687 of models for describing non-equilibrium and preferential flow and transport in the vadose
688 zone, Journal of Hydrology, 272, 14-35, 2003.
689 Tietjen, B., Jeltsch, F., Zehe, E., Classen, N., Groengroeft, A., Schiffers, K., and Oldeland, J.:
690 Effects of climate change on the coupled dynamics of water and vegetation in drylands,
691 Ecohydrology, 3, 226-237, 10.1002/eco.70, 2010.
692 Turner, D. D., Wulfmeyer, V., Berg, L. K., and Schween, J. H.: Water vapor turbulence
693 profiles in stationary continental convective mixed layers, Journal Of Geophysical
694 Research-Atmospheres, 119, 11151-11165, 10.1002/2014jd022202, 2014.
695 Uffink, G., Elfeki, A., Dekking, M., Bruining, J., and Kraaikamp, C.: Understanding the non-
696 gaussian nature of linear reactive solute transport in 1d and 2d, Transport in Porous Media,
697 91, 547-571, 10.1007/s11242-011-9859-x, 2012.
698 van Genuchten, M. T.: A closed-form equation for predicting the hydraulic conductivity of
699 unsaturated soils., Soil Sci. Soc. Am. Jour., 44, 892 - 898, 1980.
700 van Schaik, N. L. M. B., Bronstert, A., de Jong, S. M., Jetten, V. G., van Dam, J. C., Ritsema,
701 C. J., and Schnabel, S.: Process-based modelling of a headwater catchment in a semi-arid
702 area: The influence of macropore flow, Hydrological Processes, 28, 5805-5816,
703 10.1002/hyp.10086, 2014.
704 Vogel, H. J., Cousin, I., Ippisch, O., and Bastian, P.: The dominant role of structure for solute
705 transport in soil: Experimental evidence and modelling of structure and transport in a field
706 experiment, Hydrology And Earth System Sciences, 10, 495-506, 2006.
707 Wienhöfer, J., Germer, K., Lindenmaier, F., Färber, A., and Zehe, E.: Applied tracers for the
708 observation of subsurface stormflow at the hillslope scale, Hydrol. Earth Syst. Sci., 13,
709 1145-1161, doi:10.5194/hess-13-1145-2009, 2009.
710 Wienhoefer, J., and Zehe, E.: Predicting subsurface stormflow response of a forested hillslope
711 - the role of connected flow paths, Hydrology And Earth System Sciences, 18, 121-138,
712 10.5194/hess-18-121-2014, 2014.
713 Wrede, S., Fenicia, F., Martinez-Carreras, N., Juilleret, J., Hissler, C., Krein, A., Savenije, H.
714 H. G., Uhlenbrook, S., Kavetski, D., and Pfister, L.: Towards more systematic perceptual
715 model development: A case study using 3 luxembourgish catchments, Hydrological
716 Processes, 29, 2731-2750, 10.1002/hyp.10393, 2015.
717 Zehe, E., Elsenbeer, H., Lindenmaier, F., Schulz, K., and Bloschl, G.: Patterns of
718 predictability in hydrological threshold systems, Water Resources Research, 43, W07434
719 10.1029/2006wr005589, 2007.
720 Zehe, E., Blume, T., and Blöschl, G.: The principle of 'maximum energy dissipation': A
721 novel thermodynamic perspective on rapid water flow in connected soil structures, Phil.
722 Trans. R. Soc. B, 1–10, doi:10.1098/rstb.2009.0308, 2010a.
723 Zehe, E., Graeff, T., Morgner, M., Bauer, A., and Bronstert, A.: Plot and field scale soil
724 moisture dynamics and subsurface wetness control on runoff generation in a headwater in

the ore mountains, Hydrology And Earth System Sciences, 14, 873-889, 10.5194/hess-14-873-2010, 2010b.
Zehe, E., Ehret, U., Blume, T., Kleidon, A., Scherer, U., and Westhoff, M.: A thermodynamic approach to link self-organization, preferential flow and rainfall-runoff behaviour, Hydrology And Earth System Sciences, 17, 4297-4322, 10.5194/hess-17-4297-2013, 2013.
Zehe, E., Ehret, U., Pfister, L., Blume, T., Schroeder, B., Westhoff, M., Jackisch, C., Schymanski, S. J., Weiler, M., Schulz, K., Allroggen, N., Tronicke, J., van Schaik, L., Dietrich, P., Scherer, U., Eccard, J., Wulfmeyer, V., and Kleidon, A.: Hess opinions: From response units to functional units: A thermodynamic reinterpretation of the hru concept to link spatial organization and functioning of intermediate scale catchments, Hydrology And Earth System Sciences, 18, 4635-4655, 10.5194/hess-18-4635-2014, 2014.
Zimmermann, A., Schinn, D. S., Francke, T., Elsenbeer, H., and Zimmermann, B.: Uncovering patterns of near-surface saturated hydraulic conductivity in an overland flow-controlled landscape, Geoderma, 195, 1-11, 10.1016/j.geoderma.2012.11.002, 2013.

7 FIGURES

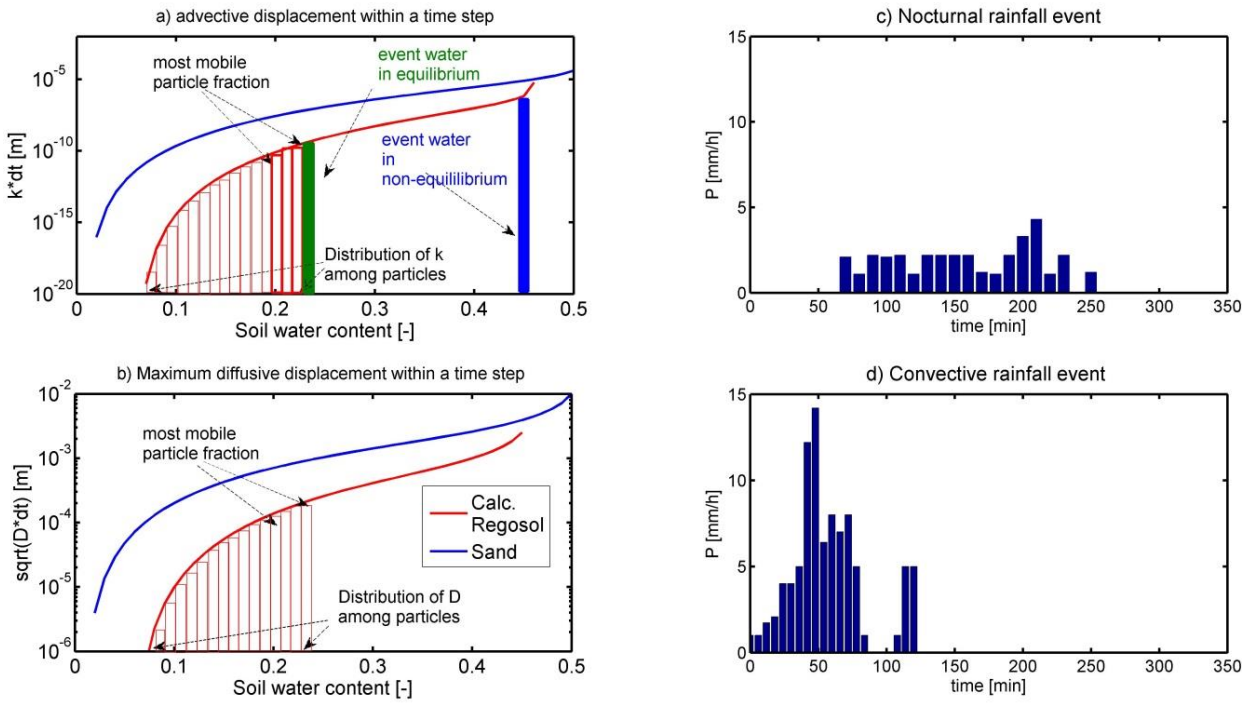

Figure 1: Advective/drift displacement of a particle k(θ) dt (panel a) and maximum diffusive displacement $(D(\theta)dt)^{0.5}$ (panel b) plotted against soil water content for the sand on limestone in the Attert catchment and the Calcaric Regosol on loess in the Weiherbach catchment. The vertical bars visualize the distribution of the D among the particles, representing water in different pore size fractions. The arrows mark the most mobile particle fraction in the five upper soil moisture classes. The red and the blue rectangle highlight the case when treating event water either as in local equilibrium and particles travel according to D((θ(t+0.5Δt)) and k((θ(t+0.5Δt)) or when they enter the coarsest pores and travel according k_s. Panel c and d present the two different rainfall events for the model testing.

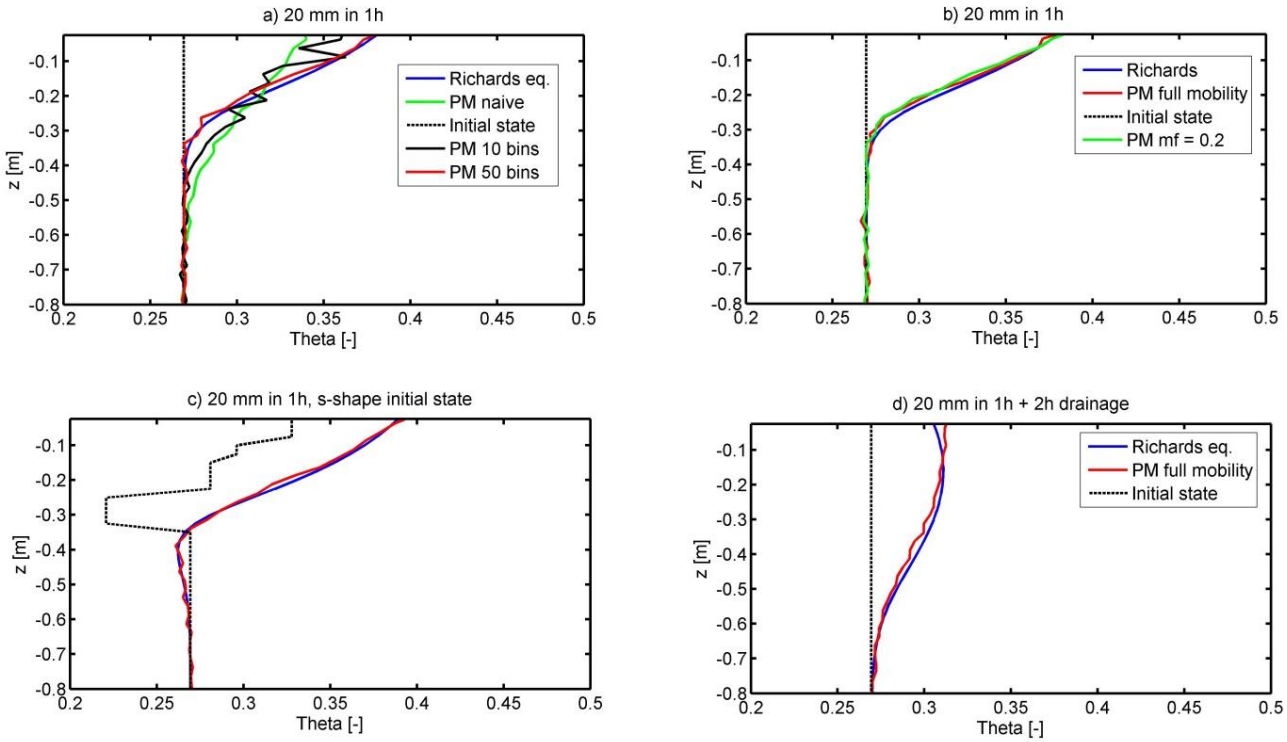

752

753 Figure 2: Final soil moisture profiles simulated for the sandy soil with the naive random walk
754 (panel a) and the particle model (PM) using different number of bins. Panel c and b compare
755 the particle model to the Richards equation for a block rain of 20 mm starting from the
756 uniform initial or the s-shaped initial state (panel b and c), mf = 0.1 denotes the mobile
757 particle fraction. Panel d) presents the same case as b after 2h of additional drainage. The
758 dashed grey line marks the initial soil moisture profiles.

759

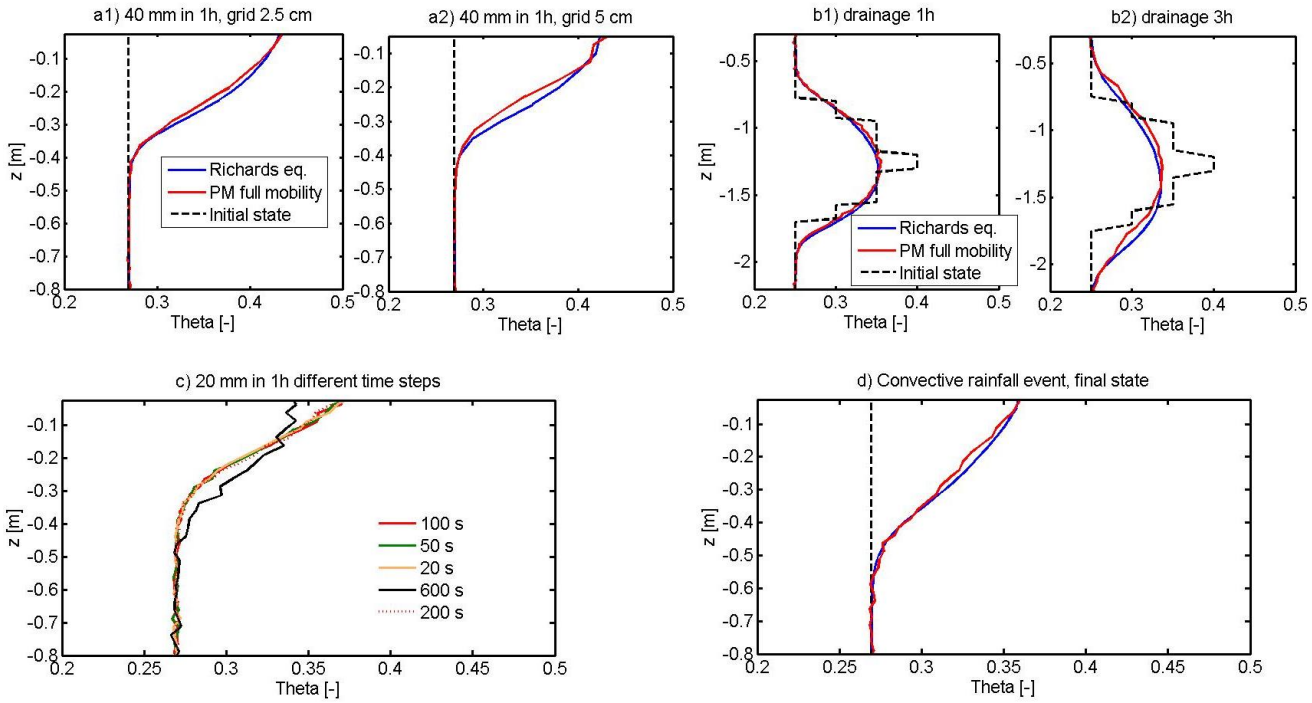

760

761 Figure 3: Final soil moisture profiles simulated for the sandy soil with full mobility model for
762 a block rain of 40 mm at two different grid sizes (Panels a1 and a2), the drainage experiment
763 starting from the clock shaped initial state (Panels b1 and b2), for a block rain of 20 mm at
764 different time steps (Panel c) and the convective rainfall event (Panel d).

765

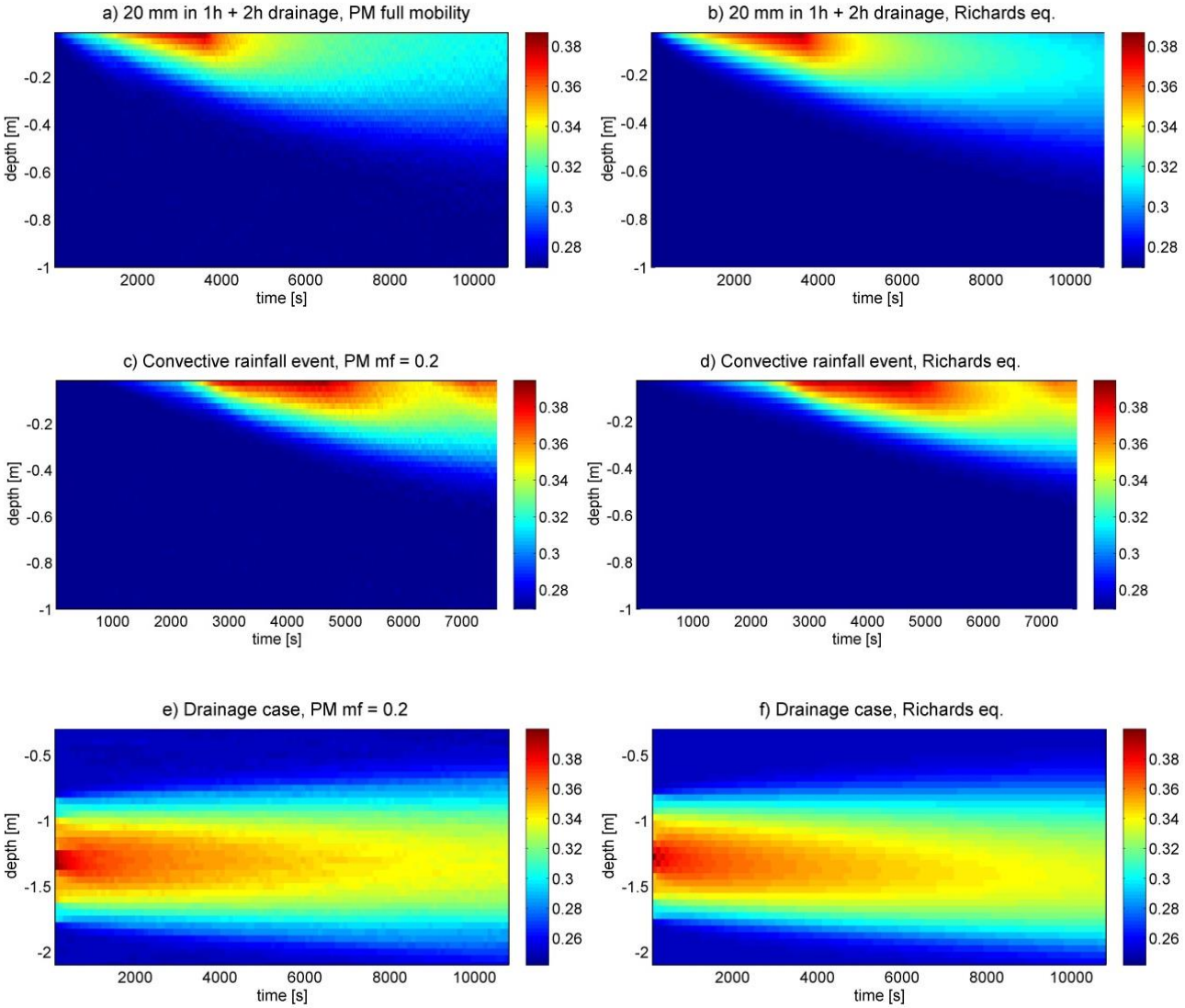

Figure 4: Time series of soil moisture simulated with the particle model (PM) and the Richards solver for the sandy soil as 2d color plots for a simulated wetting event of 20 mm in 1 h and additional 2 h of drainage (Panels a and b), the convective rainfall even (Panels c and d) and the drainage experiment (Panels e and f).

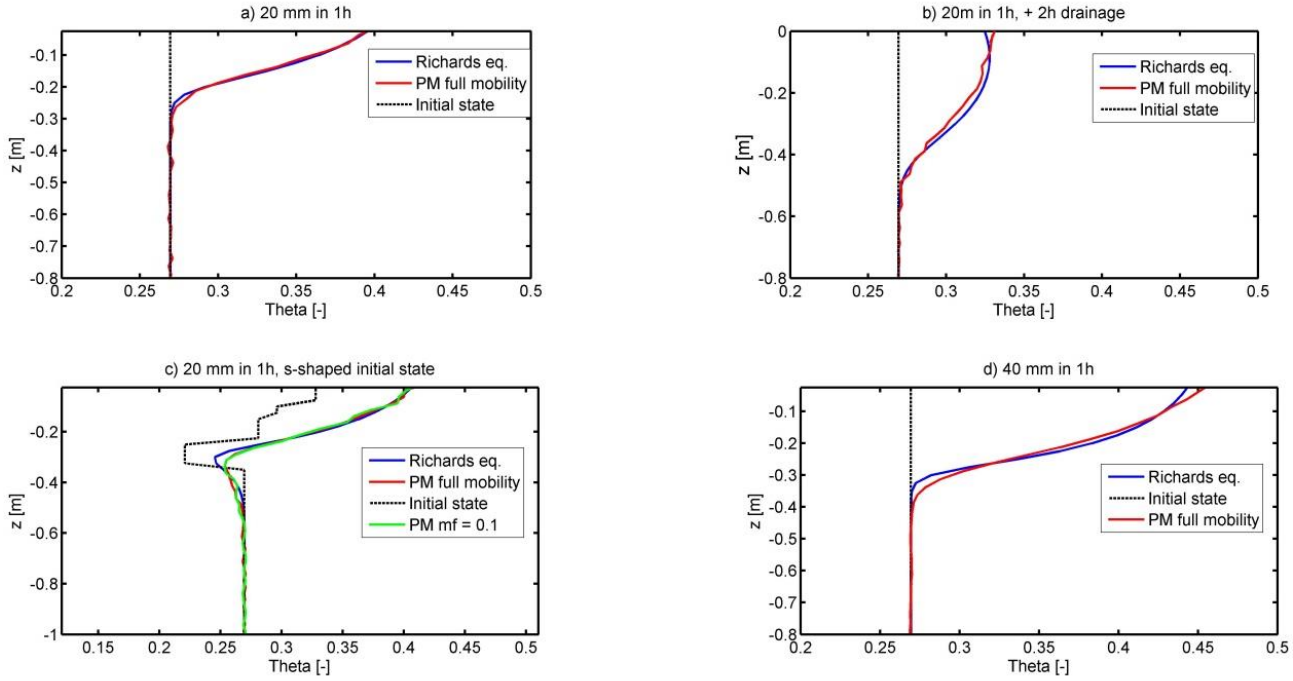

Figure 5: Final soil moisture profiles simulated with the Richards eq. and the particle model for the young silty soil on schist for the block rain of 20 mm (Panel a) and additional 2 h of drainage (Panel b), the same forcing but an s-shaped initial soil profile (Panel c), including a simulation with a mobile fraction, mf, of 10%. Panel c compares the full class approach against the Richards equation starting for a 40 mm block rain of 1h. The dashed grey line marks the initial soil moisture profiles.

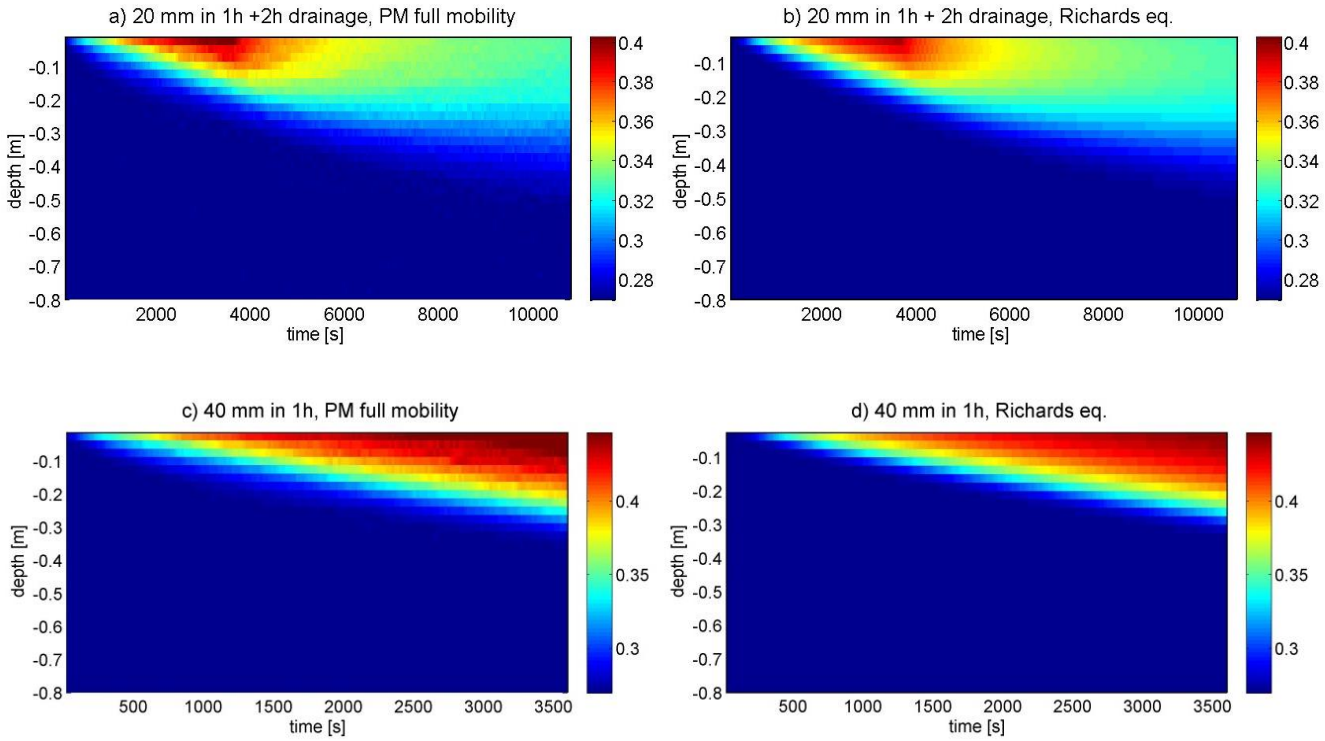

Figure 6: Time series simulated soil moisture profiles in the upper 80 cm of the young silty soil on schist for a block rain of 20 mm and 2 h of subsequent drainage (Panels a and b) and a block rain of 40 mm in 1h (Panels c and d).

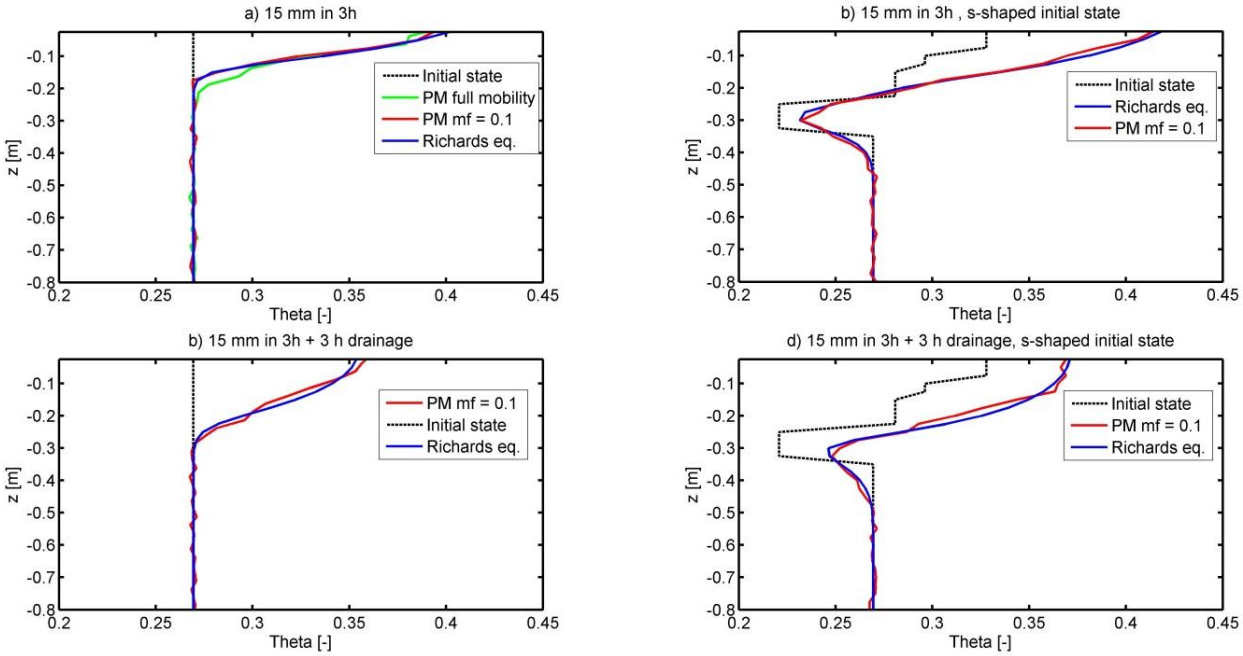

Figure 7: Final soil moisture profiles simulated for Calcaric Regosol on loess. Panels a) and b) compare the particle model in the full mobility model (solid green) and in a mobile fraction of 10 % (solid red) to the Richards solver for a 15 mm rainfall input in 3h and different initial patterns. Panels c) and d) compare the Richards solver and the particle model assuming a mobile fraction of 0.1 after 15 mm infiltration in 3 h and a subsequent drainage phase of 3 h. The dashed grey line marks the initial soil moisture profiles.

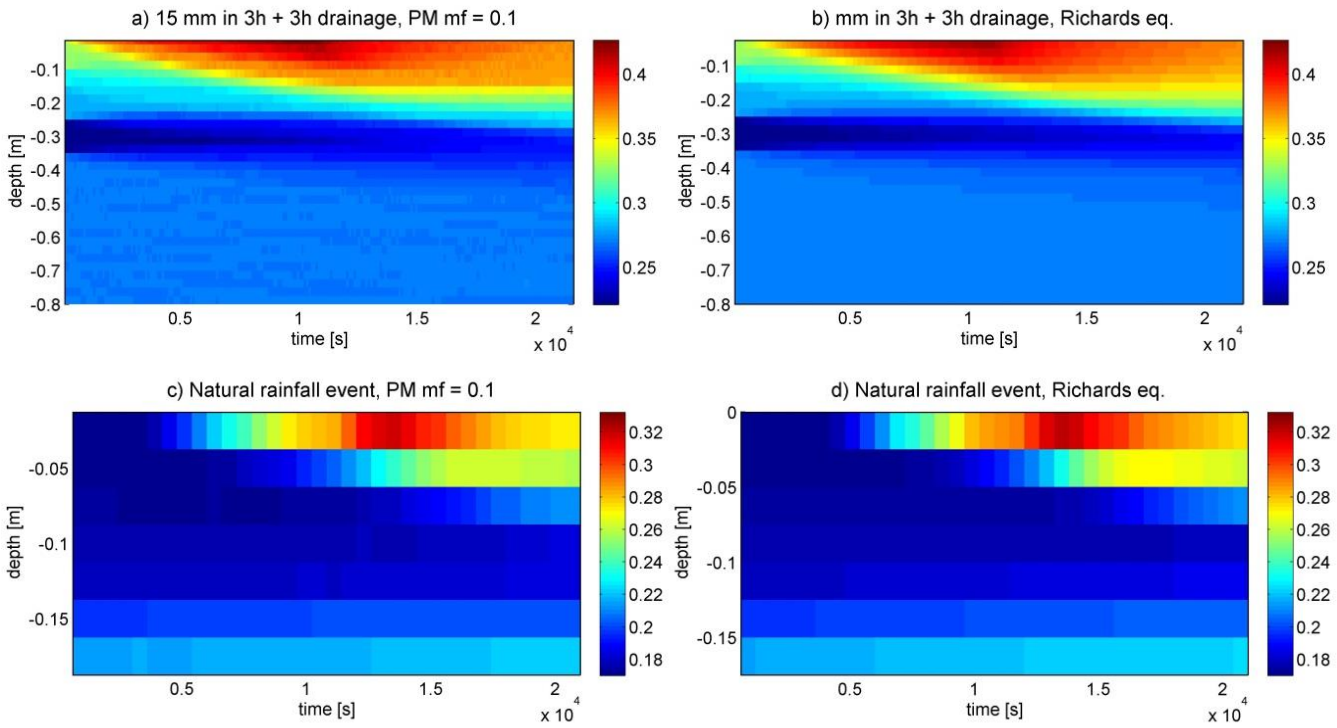

Figure 8: Time series simulated soil moisture profiles in the upper 80 cm/ 20 cm of the Calcaric Regosol on loess for a block rain of 20 mm in 1 h and 2 h of subsequent drainage (Panels a and b) starting from an s-shaped soil moisture profile and for the nocturnal rainfall event observed in May in the Weiherbach catchment (Panels c and d).

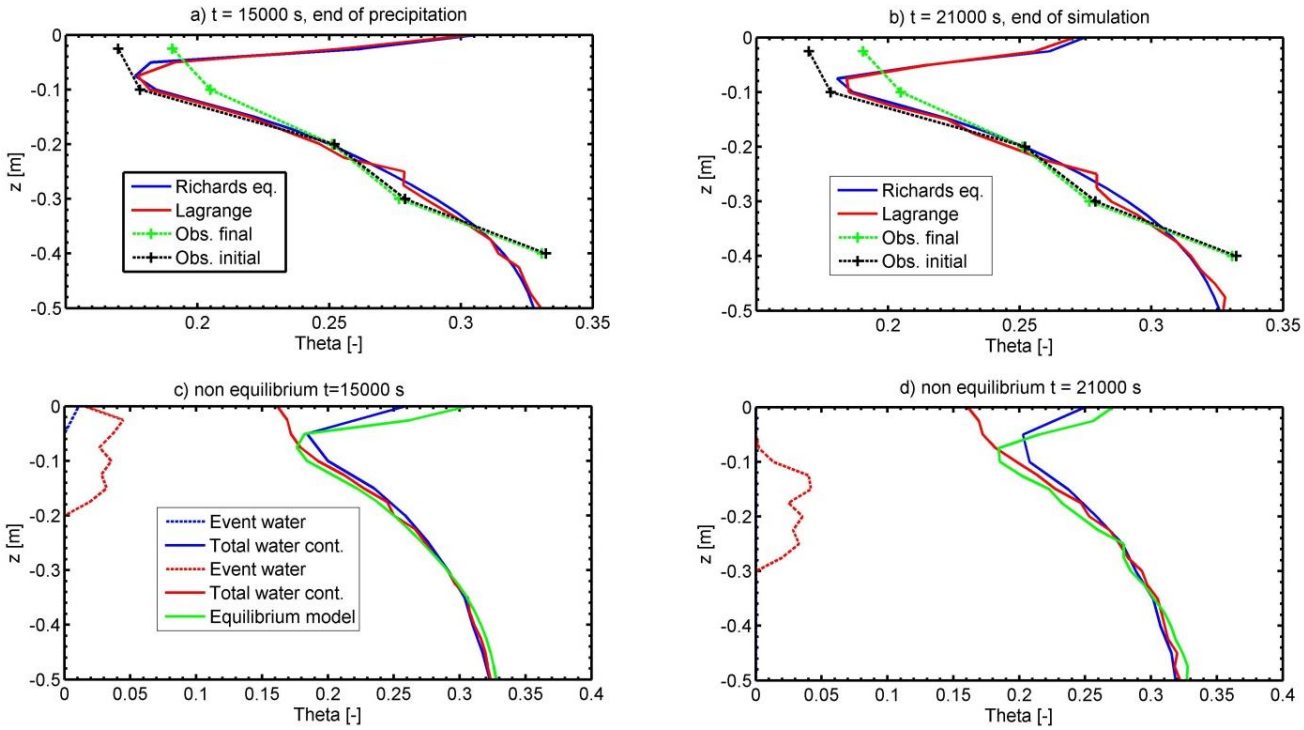

Figure 9: Soil moisture profiles simulated with the Richards equation (solid blue) and the particle model compared to observations in different depths at the end of the precipitation event (panel a), 15000s) and the end of simulation (panel b), 21000s). Initial soil moisture observations are given as black, intermediate and final observations as green crosses. Panels c) and d) present fractions of event water (dashed lines) total water content (pre-event + mixed water) for simulations assuming non-equilibrium infiltration. Blue lines correspond to t_{mix} = 4300s, red lines to t_{mix}= 7300s, the solid green line shows the soil water content simulated with equilibrium infiltration.

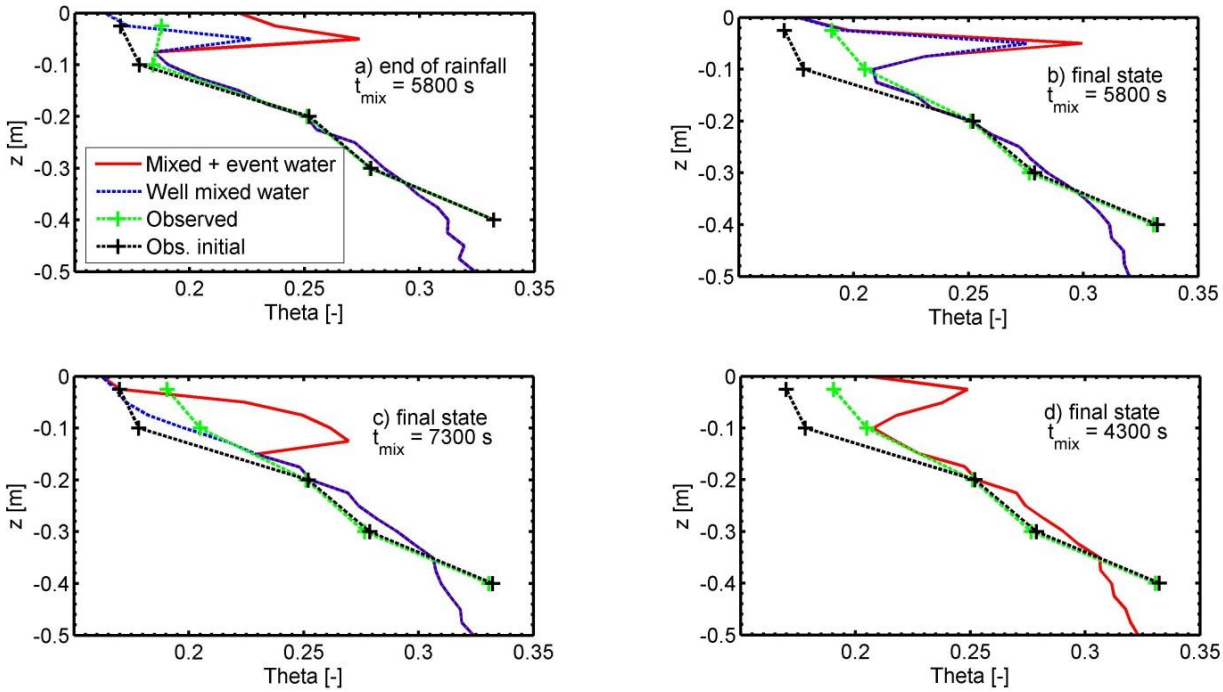

821

822 Figure 10: Non equilibrium simulations compared against observed soil moisture values, for
823 t_{mix} = 5800s after the rainfall event (panel a) and at the end of simulation (panel b). Panel c)
824 and d) present the final state for t_{mix} = 7300s or t_{mix} = 4300s, respectively.

825

8 TABLES

Table 1: Soil hydraulic parameters of the sandy soil on limestone, the young silty soil on schist and the Calcaric Regosol on loess: saturated hydraulic conductivity k_s, saturated and residual water contents θ_s, θ_r, air entry value α, shape parameter n.

Soil type	**k_s [m/s]**	**θ_s[-]**	**θ_r[-]**	**α[m^{-1}]**	**n[-]**
Sand on limestone	$2.23*10^{-4}$	0.508	0.01	4.71	1.475
Young silty soil on schist	$2.62\ 10^{-4}$	0.51	0.12	6.45	1.50
Calc. Regosol on loess	$6.0\ 10^{-6}$	0.46	0.06	1.50	1.36

833

834 Table 2: Characteristics of the numerical benchmarks: rainfall input P, initial condition θ_{ini},

835 simulation time t_{sim}

Soil type	**Wetting**	**Wetting**	**Wetting**	**Wetting &drying**
Sand	P =20 mm in 1h θ_{ini} = uniform t_{sim} =1h	P =40 mm in 1h θ_{ini} = uniform t_{sim} =1h	P =20 mm in 1h θ_{ini} = s-shape t_{sim} =1h	P =20 mm in 1h θ_{ini} = uniform t_{sim} =3h
Silty soil	P =20 mm in 1h θ_{ini} = uniform t_{sim} =1h	P =40 mm in 1h θ_{ini} = uniform t_{sim} =1h	P =20 mm in 1h θ_{ini} = s-shape t_{sim} =1h	Input: 20 mm in 1h initial con.: uniform Duration: 2h
Calc. Regosol	P =20 mm in 1h θ_{ini} = s-shape t_{sim} =1h	P =20 mm in 4h θ_{ini} = uniform t_{sim} =4h	P =15 mm in 3h θ_{ini} = s-shape t_{sim} =3h	P =15 mm in 3h θ_{ini} = uniform t_{sim} =6h

836

837

838 Table 3: Top soil and the subsoil hydraulic properties at the central meteorological station in
839 the Weiherbach catchment: saturated hydraulic conductivity k_s, saturated and residual water
840 contents θ_s, θ_r, air entry value α, shape parameter n.

Depth [m]	**k_s [m/s]**	**θ_s[-]**	**θ_r[-]**	**α[m^{-1}]**	**n[-]**
0 - 0.3	$6.0\ 10^{-6}$	0.46	0.06	1.50	1.36
> 0.3	$3.4\ 10^{-6}$	0.44	0.06	1.50	1.36

841

842

843

844